Heliyon 10 (2024) e25463

Contents lists available at ScienceDirect

Heliyon

journal homepage: www.cell.com/heliyon

Research article

Activated CD4 T cells/Tregs derived immune-metabolism signature provide precise prognosis assessment for gastric cancer and beneficial for treatment option

Junyu Huo [a], Zhen Shang [b], Xinyi Fan [c], Peng Sun [d,*]

[a] *Department of Gastrointestinal Surgery, Shandong Provincial Hospital Affiliated to Shandong First Medical University, Jinan, Shandong, 250021, China*
[b] *Medical Department of Qingdao University, Qingdao, Shandong, 266071, China*
[c] *Department of Allergy, The Affiliated Hospital of Qingdao University, China*
[d] *Department of Hepatobilary and pancreatic surgery, No. 16 Jiangsu Road, The Affiliated Hospital of Qingdao University, Qingdao, 266000, Shandong, China*

A B S T R A C T

Background: The prognostic significance of the ratio of activated CD4 T cells to Tregs infiltrating tumor tissues in gastric cancer (GC) remains unknown.
Materials and methods: For the quantification of infiltration of immune cells, the ssGSEA algorithm, which is a single sample gene set enrichment analysis, was utilized. Group A was defined as having activated CD4 T cells/Tregs >1, while group B was defined as having activated CD4 T cells/Tregs <1. To compare the overall survival (OS) of the two groups, the Kaplan-Meier survival analysis was employed. The R package 'limma' was used to identify the immune and metabolism related genes that were expressed differentially between the two groups, with a false discovery rate (FDR) less than 0.05. The risk score (RS) was constructed by combining univariate Cox regression analysis, LASSO penalized Cox regression analysis, and multivariate Cox regression analysis. The median RS was used to classify high-risk (HR) and low-risk (LR) groups.
Results: A predicted unfavorable outcome of GC was observed when the ratio of activated CD4 T cells to Tregs was less than 1. Our proposed RS was utilized for prognostic risk categorization in ten distinct independent cohorts (TCGA-STAD, n = 371; GSE84437, n = 433; GSE26253, n = 432; GSE13861, n = 65; GSE15459, n = 192; GSE26899, n = 93; GSE26901, n = 109; GSE28541, n = 40; GSE34942, n = 56; GSE62254, n = 300) and exhibited exceptional precision. In terms of tumor microenvironment (TME) and treatment strategies, compared to the LR group, the HR group was characterized by a higher infiltration levels of stromal cells, Tregs, macrophages, Tfh, mast cells, and NK cells, inclined to activated CD4 T cells/Tregs <1, and exhibited insensitivity to immunotherapy and multiple chemotherapy drugs. In relation to the potential molecular mechanism, the excessive activation of oncogenic pathways such as MAPK, hedgehog, WNT, calcium, and TGF-β signaling pathways may accelerate the malignant progression of GC by stimulating angiogenesis, promoting EMT, and altering ECM. Conversely, the overactivation of the P53 pathway is likely to inhibit tumor proliferation by regulating the cell cycle.
Conclusion: The immune-metabolism signature associated with the ratio of activated CD4 T cells and Tregs could be used to assess prognosis, TME, and treatment strategies in GC patients.

1. Background

CD8$^+$ and CD4$^+$ T cells are crucial components of the immune system's response to cancer [1]. Traditionally, the primary role of CD8$^+$ T cells has been attributed to tumor killing [2], while CD4$^+$ T cells have been regarded as supportive components of the immune

* Corresponding author.
E-mail address: psun1@qdu.edu.cn (P. Sun).

https://doi.org/10.1016/j.heliyon.2024.e25463
Received 10 July 2023; Received in revised form 16 December 2023; Accepted 27 January 2024
Available online 1 February 2024

Table 1
The clinical information for GC patients from 10 different independent cohorts.

	GSE13861	GSE15459	GSE26253	GSE26899	GSE26901	GSE28541	GSE34942	GSE62254	GSE84437	TCGA
Survival status										
alive	35	97	255	60	54	8	29	148	224	226
dead	30	95	177	33	55	32	27	152	209	145
Age										
≥65	26	108	52	35	27	15	41	134	166	202
<65	39	83	380	58	82	25	15	161	267	145
Gender										
Male	46	124	280	73	69	27	36	195	296	221
Female	19	67	152	20	40	13	20	100	137	126
Grade										
G1-2										144
G3										218
MSI										
MSS										250
MSI-L										54
MSI-H										67
Stage T										
T1-3								277	141	252
T4								21	292	95
Stage N										
N1-3								262	353	240
N0								38	80	107
Stage M										
M0	56			85	102			273		328
M1	4			7	7			27		25
AJCC stage										
I	12	31	68	11	40	1	11	30		47
II	12	29	167	18	18	6	11	94		108
III	25	72	130	27	36	12	19	95		147
IV	16	59	67	36	15	21	13	76		35
Lauren classification										
Intestinal	19	98	139	31	82		39	144		146
Diffuse	30	75	280	59	11		11	134		55
Mixed	12	18	13	2	5		4	17		14
Location										
antrum	26		226	55	56			153		139
fundus&cardia	5		54	9	13			31		47
body	31		139	29	36			107		130
Adjuvant.chemo										
Yes	49		432	67	39	40				
No	16			26	70					

system. However, recent clinical research has revealed that $CD4^+$ T cells not only express certain crucial molecules but also possess direct cytotoxic capabilities [3]. In contrast to tumor infiltrating $CD8^+$ T cells, which are susceptible to fatigue, $CD4^+$ T cells possess the ability to exert enduring anti-tumor effects, and the overall quantity of infiltrating $CD4^+$ T cells is greater in the majority of tumors [4]. Furthermore, Nabel's research group discovered that CD4+T lymphocytes could impede the progression of tumors by halting the cell cycle of tumor cells in the G1/S phase, whereas CD8+T lymphocytes lacked this capability [5]. Hence, it is crucial to unveil the anti-tumor mechanism employed by $CD4^+$ T lymphocytes.

Among the $CD4^+$ T cell family, Regulatory T cells (Tregs) are highly regarded phenotypes [6]. Regulatory T cells (Tregs) have the ability to regulate inflammation by suppressing the aberrant immune reaction triggered by excessive activation of self-reactive T cells, thus playing a crucial part in upholding autoimmune tolerance and immune balance. Additionally, it has the ability to trigger immune evasion in cancer cells and facilitate the expansion and multiplication of tumors by suppressing the anti-cancer immune reaction. This is achieved by impeding the growth, metabolism, and cytotoxicity of $CD8^+$ T cells through the release of inhibitory substances like IL-10 and TGF- β, as well as impacting the maturation of dendritic cells (DC) [7]. Tregs have also emerged as a focal point of investigation in tumor immunotherapy, utilizing the aforementioned mechanisms. Certain research has indicated that selectively removing the suppressive capabilities of Tregs (for example, through the use of CTLA-4 antibodies) can heighten the ability of effector T cells to destroy cells and enhance the effectiveness of anti-tumor treatments [8].

Gastric cancer (GC), also known as stomach cancer, is a prevalent form of primary malignancy. Currently, most patients are treated with chemotherapy, radiotherapy, and surgery, but the effectiveness still needs to be improved.The specific biological mechanism of cytotoxic $CD4^+$ T cells in GC is yet to be discovered, particularly given the various ways in which these cells exhibit anti-tumor effects in multiple preclinical models. The impact of the ratio between activated $CD4^+$ T cells and Tregs on the development of GC, as the agents that combat tumors and stimulate tumor growth, is yet to be uncovered.

2. Materials and methods

2.1. Gathering of information

Data from The Cancer Genome Atlas (TCGA) and Gene Expression Omnibus (GEO) were collected, including transcriptome and clinical data from 2091 patients with gastric cancer. The databases used were TCGA-STAD (n = 371), GSE84437 (n = 433), GSE26253 (n = 432), GSE13861 (n = 65), GSE15459 (n = 192), GSE26899 (n = 93), GSE26901 (n = 109), GSE28541 (n = 40), GSE34942 (n = 56), and GSE62254 (n = 300). Table 1 displays the clinical data of GC patients from 10 distinct independent cohorts. The mRNA expression data was standardized to the transcripts per million kilobase (TPM) format using the R software package called 'limma'. Additionally, the R package 'SVA' was utilized to eliminate any batch effects across different datasets [9]. We adhered closely to the access regulations of the openly accessible database while gathering data, and obtaining approval from the local ethics committee was unnecessary as the data was sourced from a public database [9]. The logical order of the research can be found in the graphical workflow diagram (Fig. S1).

2.2. Tumor microenvironment assessment

For the quantification of the infiltration of 23 immune cell types (ICI), the ssGSEA algorithm, which stands for single sample gene set enrichment analysis, was utilized [10]. The ESTIMATE algorithm was employed to compute the scores for the tumor microenvironment (TME), which encompassed the stromal score, immune score, estimate score, and tumor purity [11].

2.3. Characterization of molecular features

The evaluation of molecular pathways' activity was performed using the gene set variation analysis (GSVA) with the R package 'GSVA' [12]. The R package 'maftools' was used to visualize the genomics mutation landscape [13]. The R package 'limma' was used to identify the differentially expressed genes (DEGs) between subgroups, with an FDR less than 0.05 [14]. The R package 'clusterProfiler' was used to perform the Gene Ontology (GO) term annotation of the DEGs [15]. To identify the hallmarks enriched in various groups, the gene set enrichment analysis (GSEA) was employed [16]. The R package 'ConsensusClusterPlus' [17] was utilized to execute the K-means clustering algorithm.

2.4. Prognostic signature's identification and validation

The prognostic-related genes (PRGs) were chosen through univariate Cox regression analysis from the DEGs with a p-value less than 0.05. The LASSO algorithm, using the R package 'glmnet', eliminated the overfit between the PRGs by determining the penalty parameter (λ) based on the lowest partial likelihood deviance. The genes that had regression coefficients different from zero were selected using the LASSO algorithm. These genes were then included in the multivariate model based on the Akaike information criterion (AIC) using a stepwise algorithm [9,18,19]. The risk score (RS) was calculated based on the retained gene expression and their corresponding regression coefficients. The GC patients are assigned into high-risk (HR) and low-risk (LR) groups based on the median RS as the threshold. The R package 'survminer' was used to generate the Kaplan-Meier survival curve, while the 'timeROC' package was utilized to generate the time-dependent receiver operating feature curve (ROC). The validation of the signature's performance was repeatedly confirmed in every separate cohort.

2.5. Analysis of drug sensitivity

The immunotherapy response was predicted using the immunophenoscore (IPS) acquired from The Cancer Immunome Atlas (TCIA) [20]. The chemotherapy sensitivity was predicted by the R package "oncoPredict" [21].

3. Results

3.1. The prognostic importance of the infiltration ratio of activated CD4 T cells/Tregs

In 10 different independent cohorts, the overall survival (OS) of GC patients with activated CD4 T cells/Tregs >1 was relatively greater than that of those with activated CD4 T cells/Tregs <1 (Fig. 1). The signal of a poor prognosis for patients with GC was indicated by an activated CD4 T cells/Tregs <1.

3.2. The infiltration ratio of activated CD4 T cells/Tregs has an impact on the tumor microenvironment (TME), metabolic activity, and genomic stability of GC

Group A was defined as having an infiltration ratio of activated CD4 T cells/Tregs >1, while group B was defined as having an infiltration ratio of activated CD4 T cells/Tregs <1. The stromal score, immune score, and estimate score of group B were considerably greater than those of group A, while the tumor purity was notably lower than that of group A (Fig. 2A). The infiltration levels of activated CD8 T cells, Th17, and Th2 cells, apart from activated CD4 T cells, were significantly higher in group A compared to group B. Additionally, the infiltration levels of MDSC, macrophage, Th1, Tfh, mast cells, and NK cells, excluding Tregs, were significantly higher in group B compared to group A (Fig. 2B). Group A exhibited significantly higher metabolism activities compared to group B, including but not limited to nicotinate and nicotinamide metabolism, arachidonic acid metabolism, and glycerolipid metabolism (Fig. 2C). The tumor mutation burden(TMB) of group A was considerably greater than that of group B (Fig. 2D).

3.3. Immune and metabolism related genes expressed differentially between group -A and -B

A total of 612 immune-related genes that were expressed differently (DEIRGs) were found between the two groups. Out of these, 319 genes were upregulated in group B, while 293 genes were upregulated in group A (Fig. 3A). Between the two groups, a total of 484

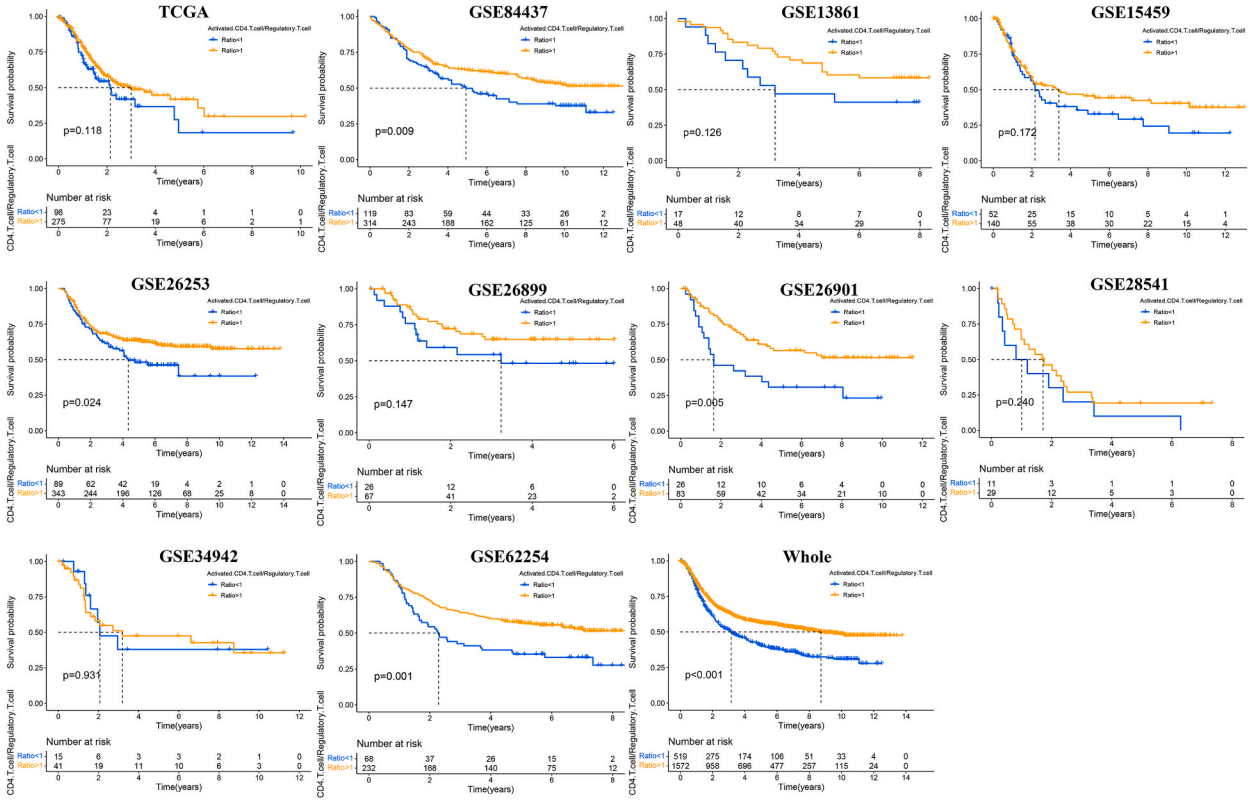

Fig. 1. The Kaplan–Meier survival analysis for GC patients with activated CD4 T cells/Tregs >1 and activated CD4 T cells/Tregs <1.

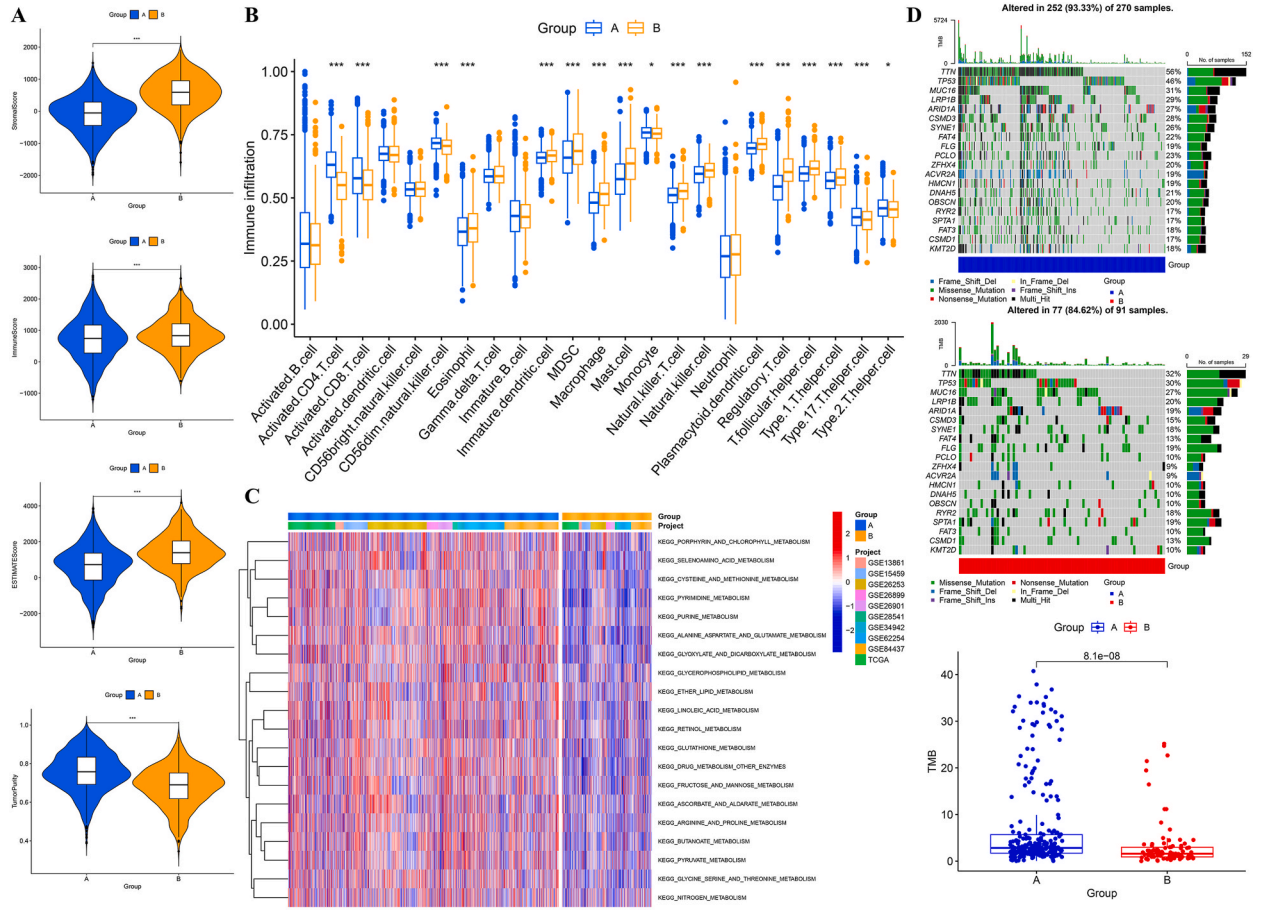

Fig. 2. The differences between group -A and -B (A) TMEscores (B) Immune cells infiltration("***", $p < 0.001$; "**", $p < 0.01$; "*", $p < 0.05$) (C) Metabolism activity (D) Somatic mutation landscape.

genes related to metabolism and expressed differentially (DEMRGs) were found. Out of these, 164 genes were upregulated in group B, while 320 genes were upregulated in group A (Fig. 3B). Using the aforementioned DEIRGs and DEMRGs, it is possible to categorize the 2091 GC individuals into three distinct groups (Fig. 3C). The OS of subtype C was considerably decreased in comparison to the other two subtypes (Fig. 3D). The subtype C with the highest mortality rate accounted for more than half of group B, far more than the other two subtypes (Fig. 4A). The stromal score, immune score, and estimate score for subtype C were notably greater compared to the other two subtypes, while having the lowest tumor purity (Fig. 4B). The three subtypes showed notable variations in the abundance of various immune cell types in terms of infiltration (Fig. 4C). The subtype C has the highest infiltration of Tregs, MDSC, macrophages, Th1, Tfh, mast cells, and NK cells, but has the lowest infiltration of activated CD4 T cells (Fig. 4D). The metabolism activities of subtype C were significantly weaker than those of the other two subtypes, subtype A has the highest metabolic activity (Fig. 4E). Nevertheless, certain cohorts did not exhibit any notable variation in prognosis among the three subtypes (Fig. 4F).

3.4. A novel immune-metabolism signature predict OS for GC

The univariate Cox regression analysis identified 584 differentially expressed genes (DEGs) that may have prognostic significance for GC (Supplementary table-1). Following the application of LASSO filtering and the selection of multivariate Cox regression analysis, a risk score (RS) was created using a combination of 54 genes (Fig. 5A and B). The detailed calculation formula of RS was provided in supplementary table-2.The RS value of 0.965 represented the median. A total of 1045 patients with RS > 0.965 were categorized as high-risk (HR), while an equal number of 1045 patients with RS < 0.965 were categorized as low-risk (LR). With the increasing RS, the patients's mortality increased obviously (Fig. 5C). The OS of GC patients in the HR group showed a notable decrease compared to the OS of GC patients in the LR group (Fig. 5D). The area under the curve (AUC) values predicted by RS for GC patients at 3 and 5 years of OS as 0.746 and 0.763, respectively (Fig. 5E).

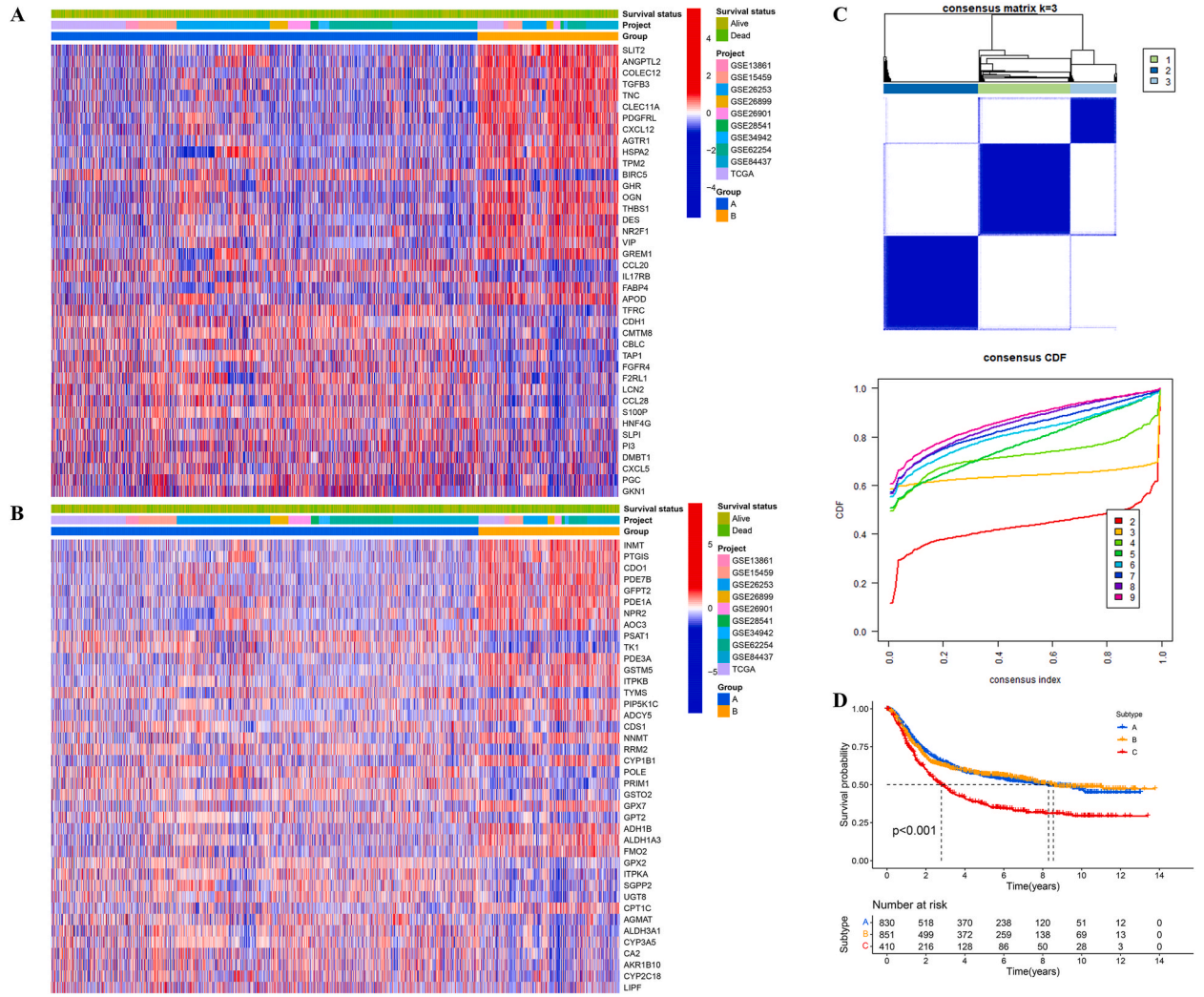

Fig. 3. Identification of DEGs between group -A and -B (A) DEIRGs (B) DEMRGs (C) Clustering analysis (D) The Kaplan–Meier survival analysis for diverse subtypes.

3.5. The signature validation was conducted in ten distinct and autonomous cohorts

In 10 separate cohorts, a common occurrence was noticed where the OS of GC patients in the HR group was notably inferior compared to the LR group (Fig. 6A–J). The stability of the signature was indicated as highly. The AUC values for the RS in predicting the OS of GC patients in the TCGA cohort were 0.645 and 0.631 at 3 years and 5 years, respectively (Fig. 6A). The values for the GSE84437 cohort were 0.772 and 0.793 (Fig. 6B).The values for the GSE62254 cohort were 0.770 and 0.763 (Fig. 6C). The values for the GSE34942 cohort were 0.654 and 0.639 (Fig. 6D). The values for the GSE28541 cohort were 0.751 and 0.958 (Fig. 6E). The values for the GSE26901 cohort were 0.766 and 0.722 (Fig. 6F). The values for the GSE26899 cohort were 0.730 and 0.731, respectively (Fig. 6G). The values for the GSE26253 cohort were 0.768 and 0.792 (Fig. 6H). The values for the GSE15459 cohort were 0.815 and 0.846 (Fig. 6I). The results for the GSE13861 cohort were 0.822 and 0.823, respectively (Fig. 6J).

3.6. Clinical correlation analysis

The Chi-square test showed that the percentage of GC patients in the HR group who had G3 poorly differentiated tumors, tumor invasion depth greater than mucosa (>T1), lymph node metastasis (N1–N3), distant metastasis (M1), diffuse lauren classification, and advanced AJCC stage were significantly higher compared to the LR group (Fig. 7). The Kaplan–Meier analysis indicated that the age, T-stage, N-stage, M-stage, AJCC stage, and lauren classification had a correlation with the OS of patients with GC (Fig. 8). Next, we categorized the GC patients into 15 clinical subgroups based on age, stage-T, stage-N, stage-M, AJCC stage, and lauren classification. The OS of HR patients was notably inferior to that of the LR patients in each subgroup (Fig. 9A–F), suggested that the signature with

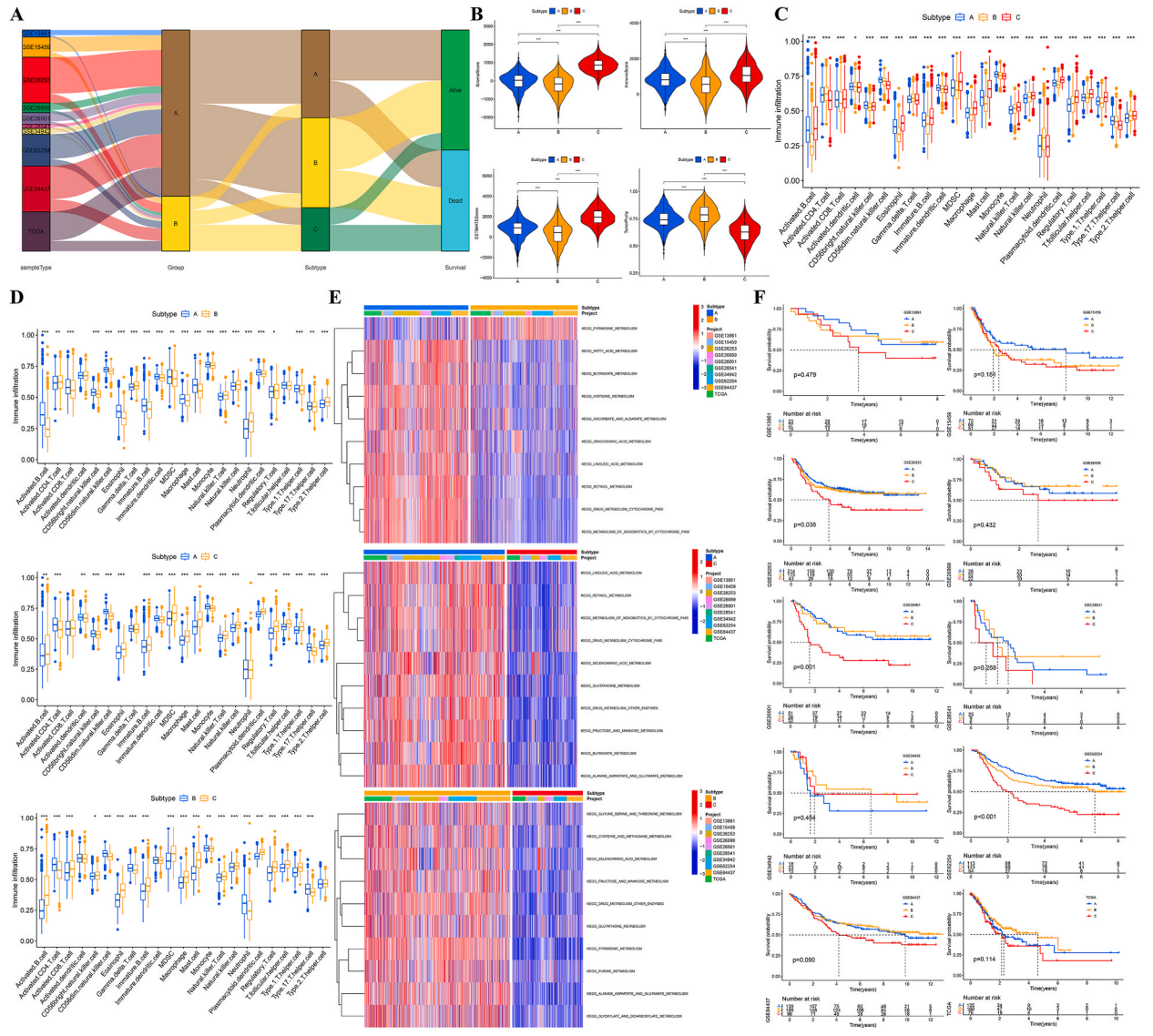

Fig. 4. The differences among three subtypes (A) Sankey diagram (B) TMEscores (C) Immune cells infiltration (D) Immune cells infiltration by pairwise comparison (E) Metabolism activity by pairwise comparison (E) The Kaplan–Meier survival analysis for diverse subtypes in 10 different independent cohorts "***", $p < 0.001$; "**", $p < 0.01$; "*", $p < 0.05$.

universal applicability.

3.7. RS could reflect the TME of GC

The RS showed a positive correlation with the stromal score and estimate score, and a negative correlation with the tumor purity. As a result, the HR group had significantly higher stromal score and estimate score compared to the LR group, but significantly lower tumor purity. Consequently, GC patients with higher stromal score and estimate score, and lower tumor purity had a poor prognosis (Fig. 10A). The LR group exhibited significantly higher infiltration levels of activated CD8 T cells, activated CD4 T cells, and Th17 cells compared to the HR group. Conversely, the HR group showed significantly higher infiltration levels of Tregs, macrophages, Tfh, mast cells, and NK cells compared to the LR group (Fig. 10B). The RS showed a positive correlation with Tregs, macrophage, Tfh, mast cells, and NK cells, while it had a negative correlation with activated CD8 T cells, activated CD4 T cells, and Th17 cells (Fig. 10C). According to TIMER, CIBERSORT, CIBERSORT-ABS, quanTIseq, xCell, MCP-counter, and EPIC algorithms, it was found that the TME of the HR group had noticeably elevated levels of cancer associated fibroblasts (CAFs), endothelial cells, and macrophage M2 compared to the LR group (Fig. 11A). The RS showed a positive correlation with the abundance of CAFs, endothelial cells, and M2 macrophages (Fig. 11B).

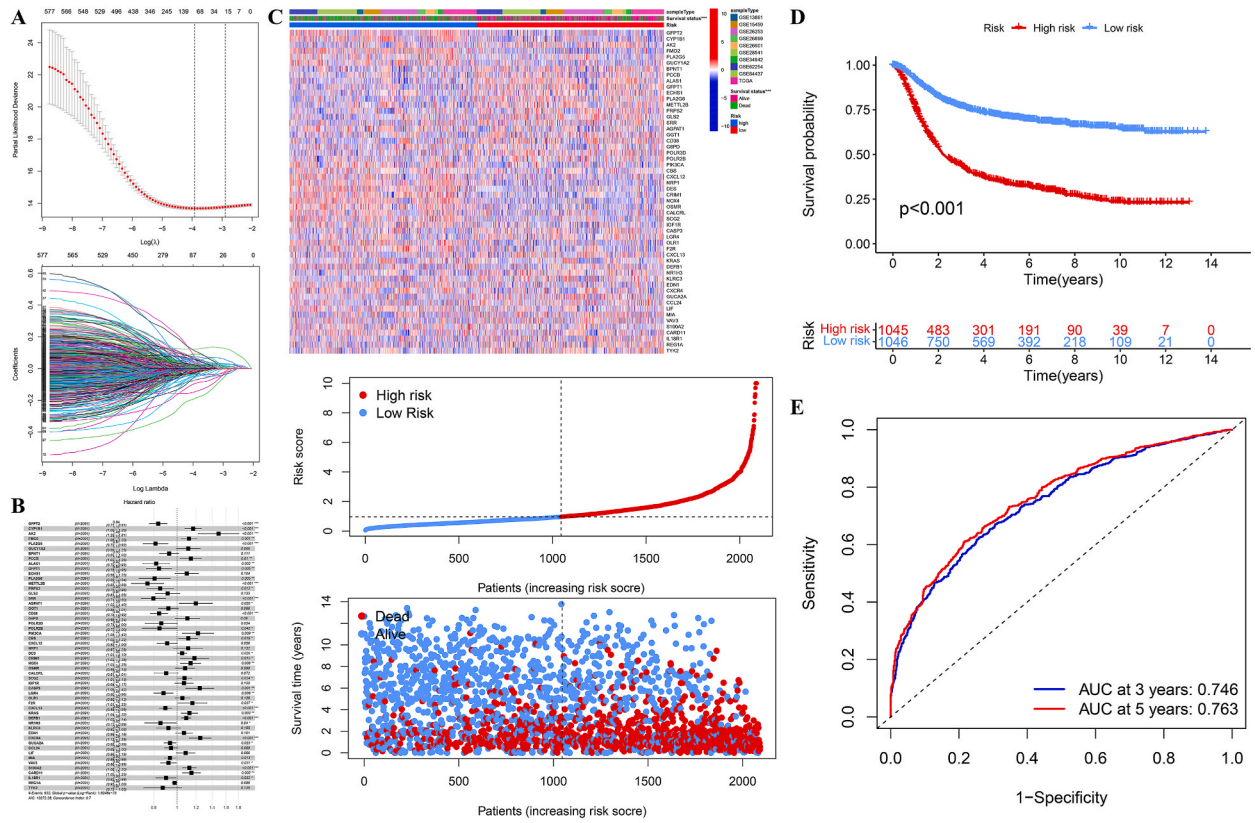

Fig. 5. Construction of the risk score (A) LASSO penalized Cox regression analysis (B) Multivariate Cox regression analysis (C) The heatmap, risk score, and survival status distribution (D) The Kaplan–Meier survival curve (E) The time-dependent ROC curve.

3.8. Molecular characteristics for different risk groups

In the LR group, the TMB was considerably greater compared to the HR group, and there was a negative correlation between RS and TMB. Additionally, GC patients with low-TMB in the HR group had the poorest prognosis (Fig. 12A). The LR group had a significantly higher stemness index (mRNAsi) compared to the HR group. Additionally, there was a negative correlation between RS and mRNAsi. Furthermore, the prognosis of GC patients with low mRNAsi in the HR group was the worst (Fig. 12B). According to the Chi-square test, the LR group had a significantly higher proportion of GC patients with activated CD4 T cells/Tregs >1 compared to the HR group (Fig. 12C). GSVA indicated that in the HR group, MAPK signaling and the Hedgehog signaling pathways were more active than in the LR group, whereas metabolism and P53 signaling pathways were weaker (Fig. 12C). The DEGs that were upregulated in the HR group primarily participated in the organization of the extracellular matrix (ECM), organization of the extracellular structure, and organization of the external encapsulating structure, among others (Fig. 12D). The HR group showed a highly enrichment of the epithelial-mesenchymal transition (EMT) and angiogenesis hallmarks, as revealed by GSEA (Fig. 12D). The DEGs that were upregulated in the LR group primarily participated in the biogenesis of ribonucleoprotein complexes, ribosomes, and the production of precursor metabolites and energy, among other functions (Fig. 12E). The LR group showed a highly enrichment of the E2F targets and G2/M checkpoint hallmarks, as revealed by GSEA (Fig. 12E).

3.9. Immunotherapy and chemotherapy were better suited for patients with a low risk level of complications

The LR group exhibited markedly elevated expression levels of CD274(PDL1), CTLA4, PDCD1, TIGIT, and LAG3 compared to the HR group (Fig. 13A). The IPS of the LR group was notably greater than that of the HR group (Fig. 13B), it was proposed that the LR group exhibited a superior reaction to immune checkpoint inhibitors (ICIs). In the LR group, the IC50 values of various chemotherapy drugs, including 5-Fluorouracil, Camptothecin, Docetaxel, Cisplatin, Oxaliplatin, and Paclitaxel, were notably lower compared to the HR group (Fig. 13C).

4. Discussion

Since 2010, tumor immunotherapy has developed rapidly, and therapies primarily based on ICIs have been proven to produce

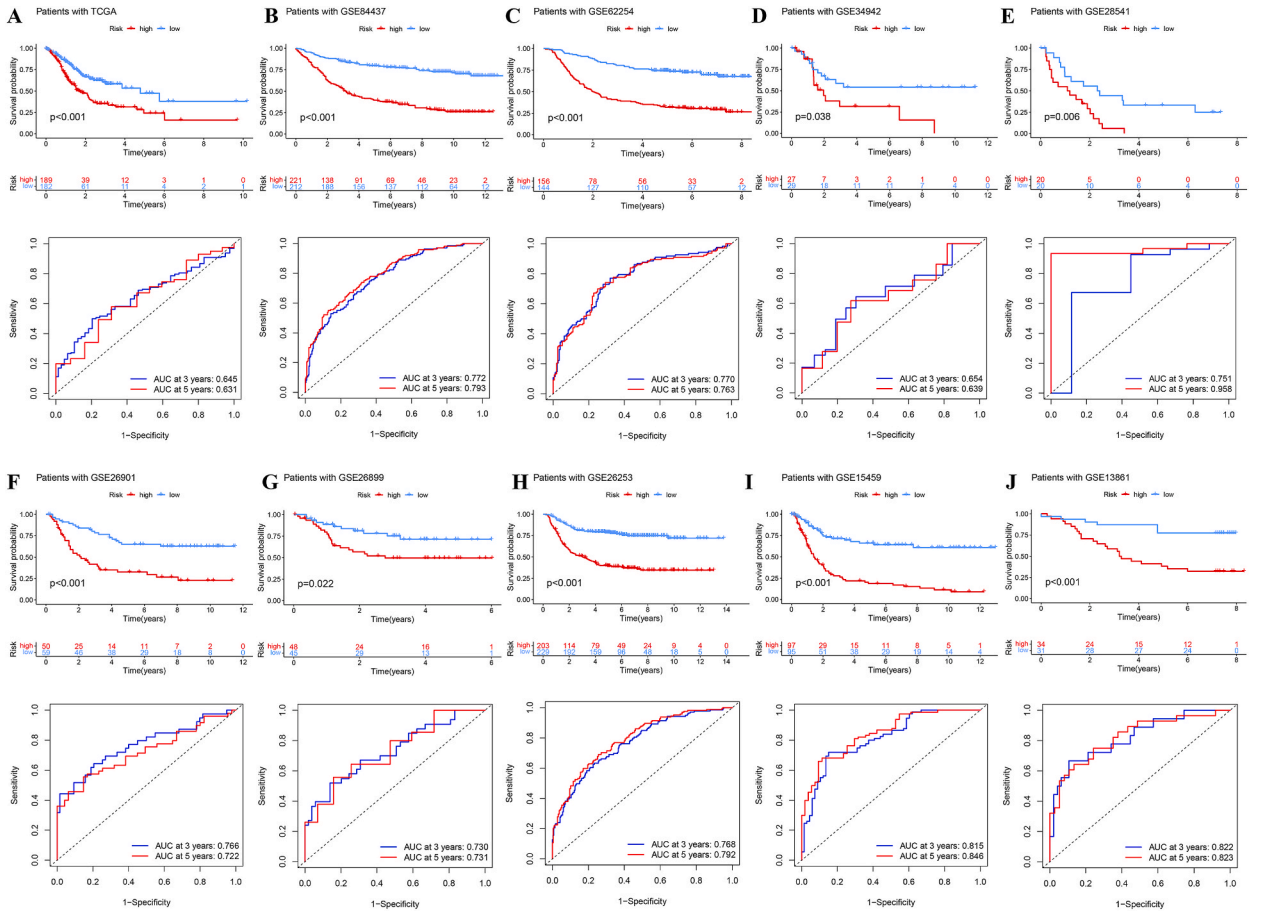

Fig. 6. Validation of the prognostic signature in 10 different cohorts Construction of the risk score (A) TCGA (B) GSE84437 (C) GSE62254 (D) GSE34942 (E) GSE28541 (F) GSE26901 (G) GSE26899 (H) GSE26253 (I) GSE15459 (J) GSE13861.

significant antigen-specific immune responses [22]. Increasing the initial activation level of T cells is a crucial determinant for the success or failure of this therapy [23]. In the field of tumor immunology, $CD4^+$ T cells have been given less focus compared to $CD8^+$ T cells [24]. Recent research has validated that $CD4^+$ T cells might exhibit more potent immune responses against tumors compared to $CD8^+$ T cells [25]. Additionally, $CD4^+$ T cells can independently generate anti-tumor immune responses without depending on $CD8^+$ T cells [26].Various types of preclinical and clinical evidence suggest that the recognition of cancer antigens by $CD4^+$ T cells is crucial for immunotherapy and can offer clinical advantages to individuals with cancer [27]. All of these factors suggest that investigating the therapeutic potential of $CD4^+$ T cells in combating tumors holds great importance in clinical settings. Currently, there is a growing focus on the involvement of $CD4^+$ T cells in tumor immunity; however, the precise explanation for its activation mechanism remains elusive [28]. According to researchers, the elimination of Treg cells can enhance the anti-cancer effect of $CD4^+$ T cells, indicating that Treg hinders the activation of $CD4^+$ T cells [29]. In hepatocellular carcinoma, which is also a digestive tract tumor, targeting Tregs could repair the unbalance of immune tolerance and benefit patients from the application of ICIs [30]. Hence, it is our conjecture that the prognosis of GC could be influenced by the activation of $CD4^+$ T cells/Tregs.

In 10 separate cohorts ($n = 2091$), it was observed that the OS of GC patients with higher levels of activated CD4 T cells/Tregs (>1) (group A) was comparatively greater than the OS of GC patients with lower levels of activated CD4 T cells/Tregs (<1) (group B). This suggests that this occurrence is common in GC, although it has not been given due attention as a universal phenomenon. Hence, a low ratio of activated CD4 T cells/Tregs infiltrating the tumor was found to be an adverse prognostic factor for GC patients, marking a significant discovery at the onset of our investigation. To uncover its underlying causes, we compared the TME, molecular pathway activities, and somatic mutation landscape of the two groups. The TMEscores, which consist of stromal score, immune score, and estimate score, were markedly elevated in group B compared to group A. This indicates that the overall presence of non-tumor cell elements in TME, including stromal cells and immune cells, is considerably higher in group B than in group A. Consequently, this disparity in cell composition is responsible for the lower tumorpurity observed in group B. Nevertheless, it should be noted that the enhanced presence of various immune cell types was not observed in group B. In addition to the presence of activated CD4 T cells, we noticed that the levels of infiltrated activated CD8 T cells, Th17, and Th2 cells in group A were considerably greater compared to group B. Hence, the comprehensive evaluation of the tumor microenvironment (TME) in GC patients based on the relative abundance of a

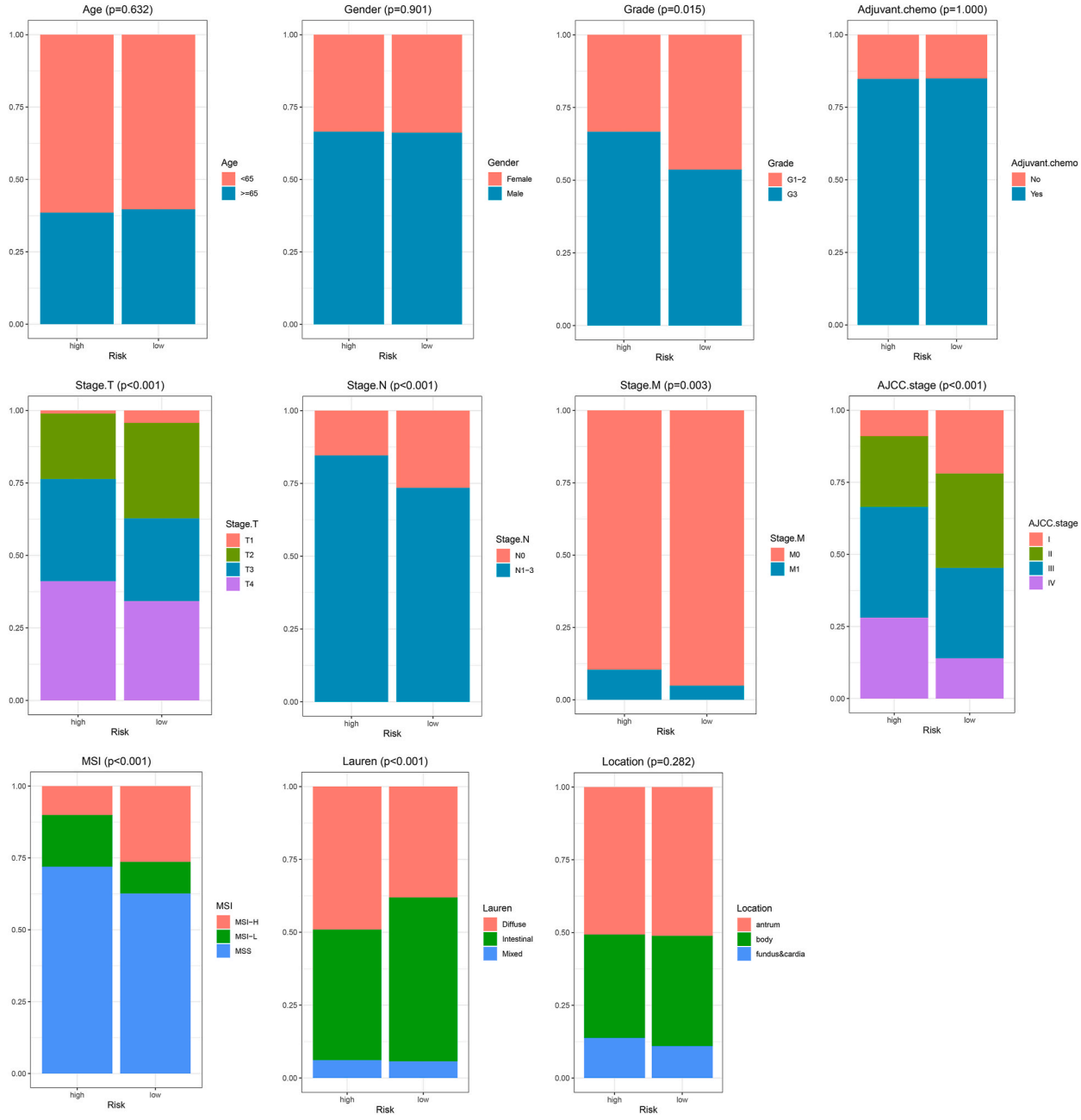

Fig. 7. Comparison of clinical features between HR and LR groups.

particular immune cell infiltration was inadequate. Group A exhibited significantly higher metabolic activity compared to group B, particularly in pyrimidine and purine metabolism, suggesting potential variations in the cell cycle between the two groups. Given the notable disparity in TMB between group A and group B, it is plausible to hypothesize that variations in genomic stability could potentially influence the expression of immune and metabolism-related genes in these two groups. As expected, we obtained 612 DEIRGs and 484 DEMRGs by compring the two groups. Significantly, the 2091 patients with GC could be categorized into three subgroups based on the aforementioned DEGs, and the OS of subtype C was notably decreased in comparison to the other two subtypes. This suggests that these DEGs hold significant significance in predicting the prognosis of GC. The prognostic value of the infiltration ratio of activated CD4 T cells/Tregs was confirmed in more than 50 % of patients belonging to subtype C. The stromal score, immune score, and estimate score of subtype C, which has a poor prognosis, were considerably higher than the scores of the other two subtypes. However, subtype C also had the lowest tumor purity, aligning with group B where activated CD4 T cells/Tregs is less than 1.In comparison to the other two subtypes, subtype C exhibits the greatest degree of Treg infiltration and the lowest degree of activated CD4

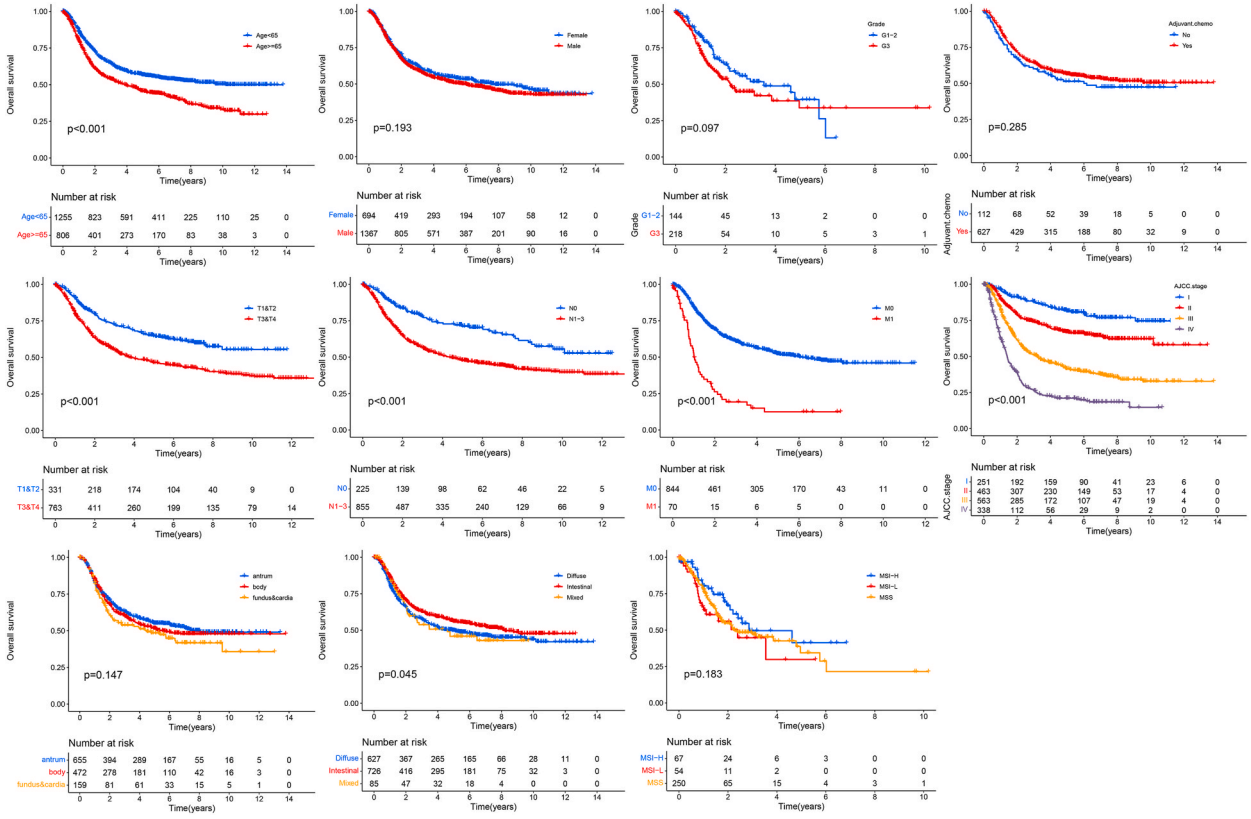

Fig. 8. The Kaplan–Meier survival analysis for clinical indicators.

T cell infiltration.The levels of Tregs and activated CD4 T cells of subtype B had higher infiltration compared to subtype A, however, there was no variation in the prognosis between the two subtypes. Hence, accurately assessing the prognosis of GC solely based on the infiltration level of one immune cell type might pose challenges, emphasizing the importance of measuring the ratio of activated CD4 T cells to Tregs. The metabolic functions of subtype C were considerably less potent compared to the other two subtypes, suggesting that a high metabolic activity served as an indicator for a favorable prognosis in GC. Nevertheless, the utilization of subtype as a means to assess the risk of GC prognosis appears inadequate, as our analysis revealed no statistically significant variation in prognosis across the three subtypes in certain independent cohorts, including GSE13861, GSE28541, and GSE34942, among others.

In order to enhance the model's performance, we utilized a combination of univariate Cox regression analysis, LASSO, and multivariate Cox regression analysis to identify the PRGs. In the end, a predictive model consisting of 54 genes was developed to estimate the OS of GC patients.The OS of patients with GC significantly decreased as the RS increased. It is crucial to emphasize that there were notable disparities in OS between the HR group and the LR group across the 10 separate cohorts. Specifically, the HR group exhibited a clear reduction in OS compared to the LR group. All AUC values for the RS predict the 5-year OS, except for TCGA and GSE34942, surpassed 0.72. From a clinical perspective, the HR group demonstrated a higher tendency towards poor differentiation (G3), deeper tumor invasion beyond the mucosa (>T1), lymph node metastasis (N1–N3), distant metastasis (M1), diffuse lauren classification, and advanced AJCC stage compared to the LR group. These findings may contribute to the understanding of the unfavorable prognosis observed in the HR group. However, we discovered that despite the absence of an age disparity between the two groups, the OS of patients aged over 65 years was significantly lower compared to patients aged below 65 years. In addition to age, the OS of GC patients was also associated with stage-T, stage-N, stage-M, AJCC stage, and lauren classification, which aligns with the conventional viewpoint. The OS of the HR group was significantly lower than the LR group in every subgroup categorized by clinical prognostic indicators, which encompassed age, stage-T, stage-N, stage-M, AJCC stage, and lauren classification. Hence, these findings indicated that the RS exhibits a high level of precision and dependability in forecasting the OS of patients with GC, surpassing conventional clinical markers.

The stromal score of the HR group was notably greater than that of the LR group, while there were no disparities in the immune score between the two groups. The HR group had a significantly higher percentage of patients with CD4 T cells/Tregs <1 compared to the LR group. The prognosis of GC is determined by the absolute content of stromal cells and the relative infiltration ratio of various immune cell types, as indicated by this data. The LR group exhibited a notable increase in metabolic activity in comparison to the HR group, thereby validating that diminished metabolic activity served as an indicator of unfavorable prognosis in patients with GC. Regarding the molecular mechanism, the HR group displayed more robust functions in the MAPK, Hedgehog, WNT, Calcium, and TGF-

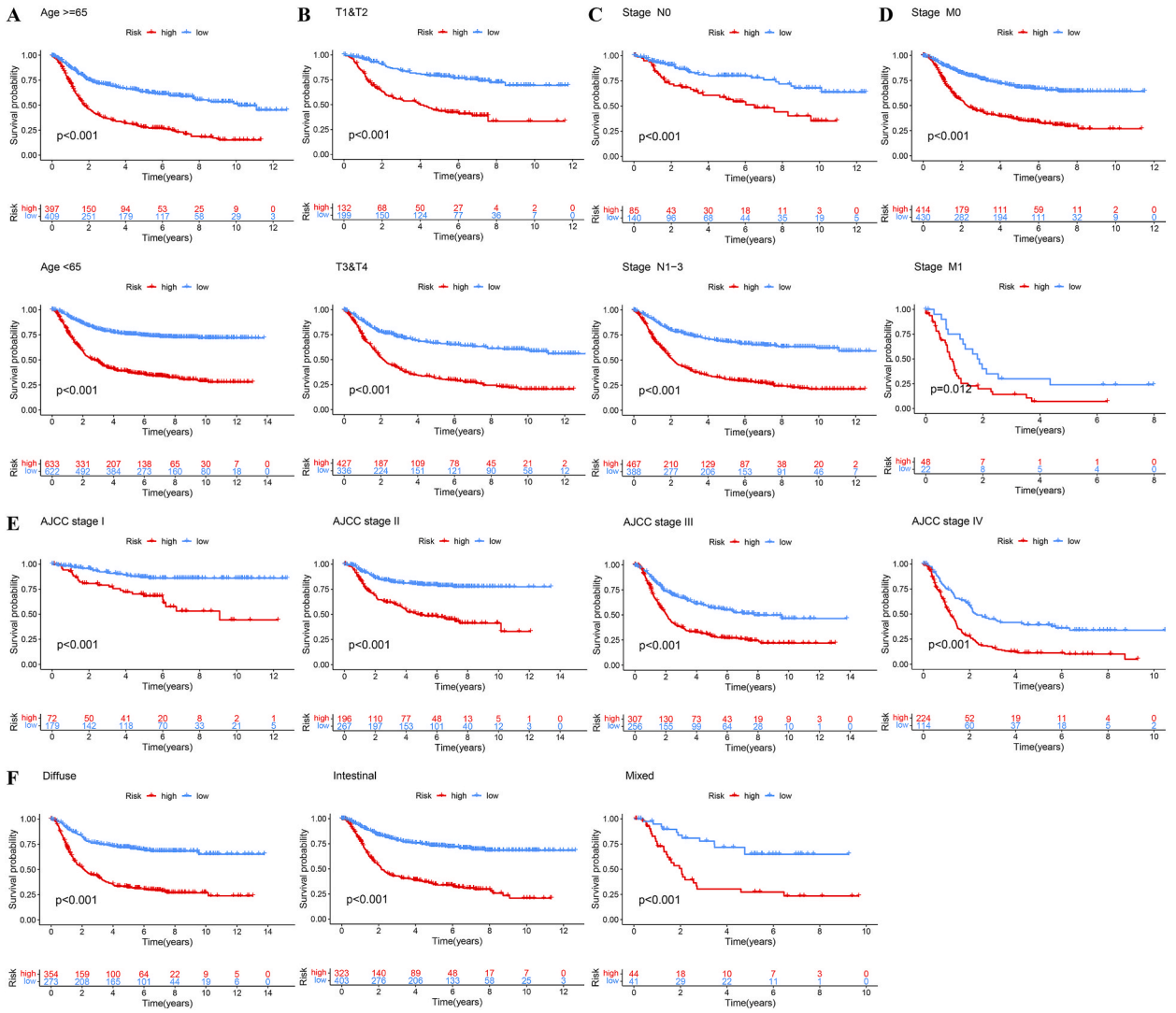

Fig. 9. Subgroup analysis for prognostic related clinical indicators.

β signaling pathways. The upregulated DEGs in the HR group primarily participated in the organization of ECM structure, and GSEA analysis indicated an enrichment of EMT and angiogenesis hallmarks in the HR group. Conversely, the LR group demonstrated a higher activity in the P53 signaling pathway, with the upregulated DEGs associated with DNA replication. GSEA analysis revealed an enrichment of G2/M checkpoint hallmarks in the LR group.We hypothesized that the excessive activation of cancer-causing pathways, including MAPK, Hedgehog, WNT, Calcium, and TGF-β signaling pathways, could potentially expedite the malignant advancement of GC through the stimulation of angiogenesis, facilitation of EMT, and alteration of ECM. Conversely, the excessive activation of the P53 pathway was expected to impede tumor growth by controlling the cell cycle. The discovery of these findings offers fresh perspectives on the development of GC. The LR group showed greater sensitivity to immunotherapy and chemotherapy compared to the HR group when selecting treatment options. The LR group's superior response to ICIs may be attributed to its elevated levels of immune checkpoints, including CD274 (PDL1), CTLA4, PDCD1, TIGIT, and LAG3, among others, as well as a higher TMB. As a result, the HR team has an unfavorable outlook and a lack of successful therapy, making them a patient group that requires heightened attention in a clinical setting.

Based on our research, patients with GC who have a poor prognosis display the following characteristics. Clinically, these patients are primarily characterized by being poorly differentiated (G3), having tumor invasion depth beyond the mucosa (>T1), lymph node metastasis (N1–N3), distant metastasis (M1), diffuse lauren classification, and an advanced AJCC stage. Regarding the TME, these patients exhibit a high infiltration of stromal cells, and the ratio of activated CD4 T cells to Tregs in tumor tissues is less than 1. In terms of molecular features, these patients show suppressed metabolic activity, while the MAPK, Hedgehog, WNT, Calcium, and TGF-β signaling pathways are overactivated. When it comes to treatment response, these patients do not respond well to immunotherapy and chemotherapy. Identifying these predictive characteristics will give us insights for creating novel approaches for treating GC. We

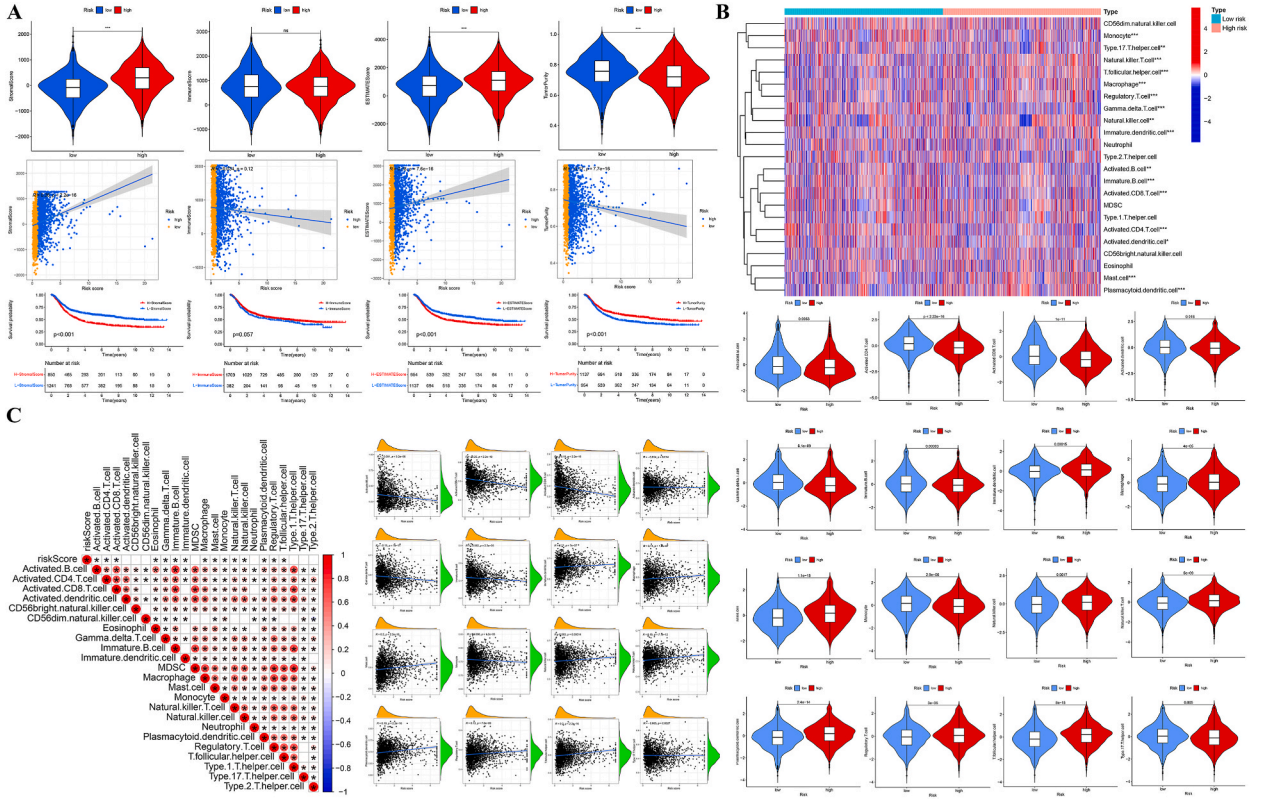

Fig. 10. Comparison of TME between HR and LR groups (A) TMEscores (B) Immune cells infiltration difference (C) Correlation analysis between the RS and abundance of immune cells infiltration.

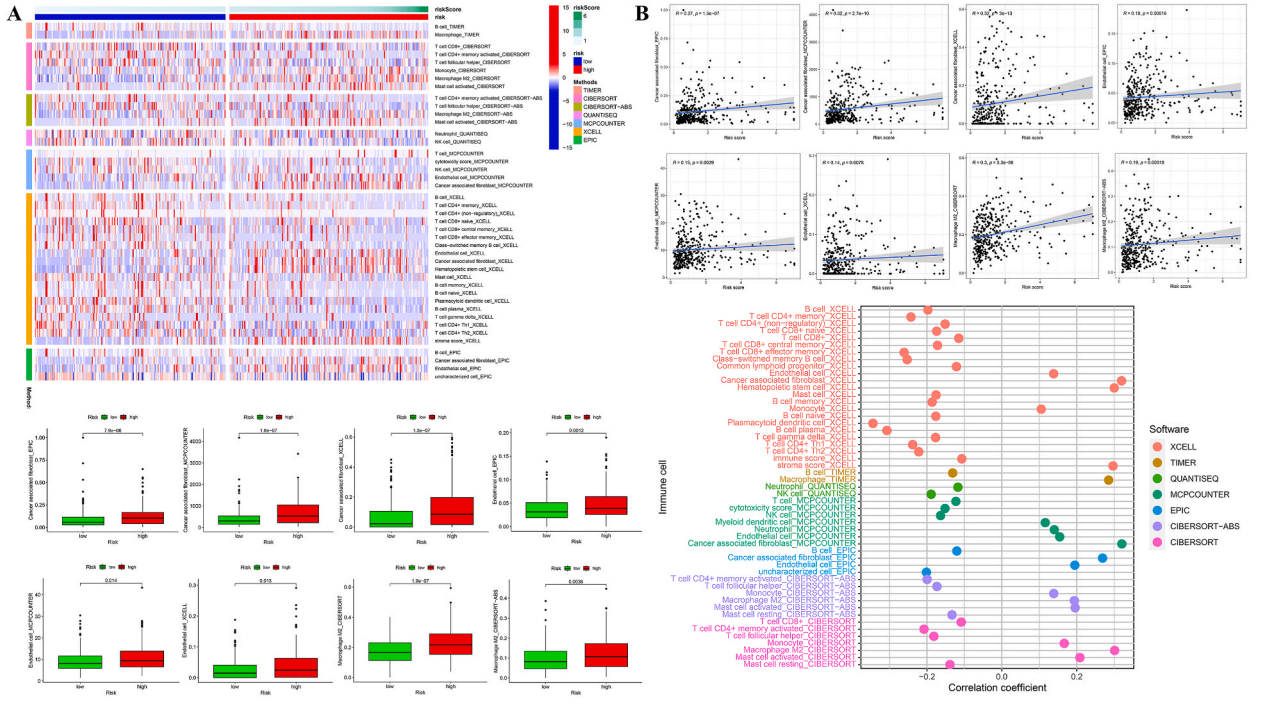

Fig. 11. Immune cells infiltration quantified by TIMER, CIBERSORT, CIBERSORT-ABS, quanTIseq, xCell, MCP-counter and EPIC algorithms (A) Immune cells infiltration difference analysis (B) Immune cells infiltration correlation analysis.

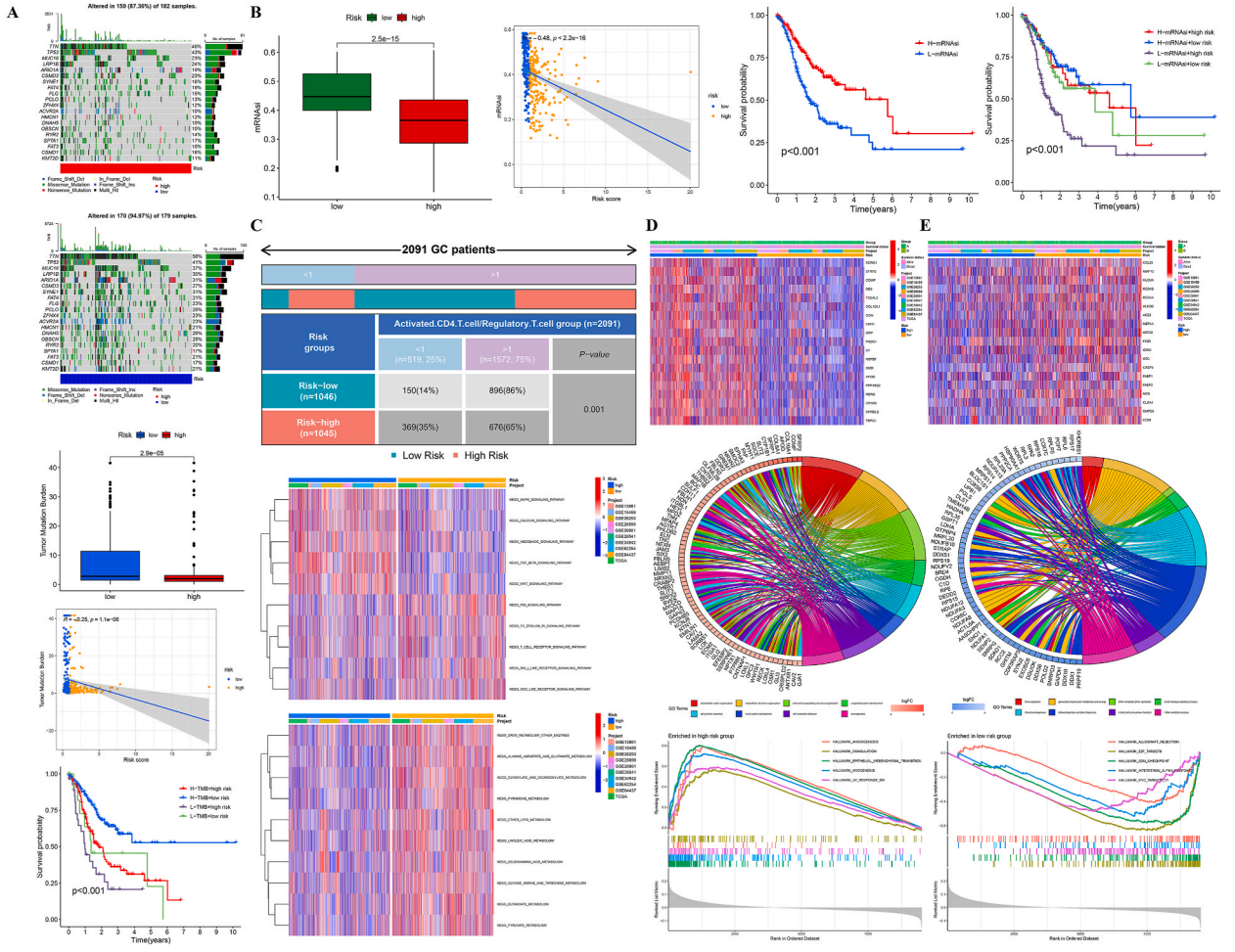

Fig. 12. Comparison of molecular characteristics between HR and LR groups (A) Somatic mutation landscape (B) Stemness index (mRNAsi) (C) Molecular pathway activity (D) Hallmarks and DEGs upregulated in the HR group (E) Hallmarks and DEGs upregulated in the LR group.

suggest assessing the proportionate infiltration rate of immune cells in clinical settings to assess prognosis, rather than solely focusing on the absolute abundance of a particular immune cell type.

In our analysis of the entire research process of this paper, our attention was directed towards the occurrence of CD4 T cells/Tregs<1, which is associated with an unfavorable outcome in GC. Group A was defined as having activated CD4 T cells/Tregs >1, while group B was defined as having activated CD4 T cells/Tregs <1. Due to notable variations in the immune micoenvironment and metabolism observed between the two groups, we successfully identified the DEIRGs and DEMRGs. Using these DEGs, we performed cluster analysis and constructed RS, gradually identifying the features associated with unfavorable prognosis in GC. In particular, the RS we suggested was applicable for the classification of prognostic risk in 10 distinct independent groups, demonstrating a high level of accuracy. This serves as a crucial foundation for the implementation of clinical translation.

5. Conclusion

A prognosis of GC is predicted to be poor when the number of activated CD4 T cells/Tregs is less than 1. Taken from this clue, we developed and validated a immune-metabolism signature, which was applicable for the prognosis, TME, and treatment strategies assessment in GC.

Ethics approval and consent to participate

Not applicable.

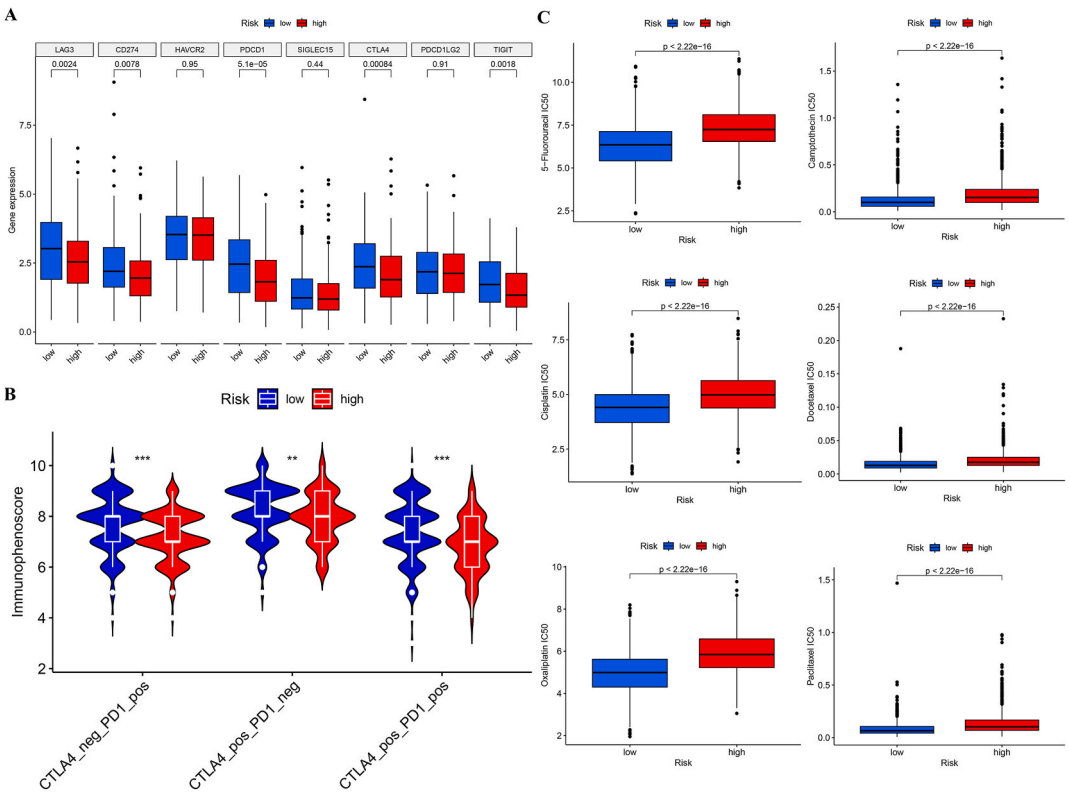

Fig. 13. Drug sensitivity prediction (A) The expression difference of immune checkpoints between HR and LR groups (B) Comparison of IPS between HR and LR groups("***", $p < 0.001$; "**", $p < 0.01$; "*", $p < 0.05$) (C) Chemotherapy drugs sensitivity prediction.

Consent for publication

Not applicable.

Availability of data and material

The datasets analysed for this study were obtained from The Cancer Genome Atlas (TCGA,https://portal.gdc.cancer.gov/), Gene Expression Omnibus(GEO, https:// www.ncbi.nlm.nih.gov/geo/), and The Cancer Immunome Atlas(TCIA, https://tcia.at/home).

Funding

This study did not receive any funding in any form.

CRediT authorship contribution statement

Junyu Huo: Conceptualization, Data curation, Formal analysis, Investigation, Methodology, Software, Supervision, Validation, Visualization, Writing – original draft, Writing – review & editing. **Zhen Shang:** Data curation, Investigation, Writing – review & editing. **Xinyi Fan:** Data curation, Investigation, Writing – review & editing. **Peng Sun:** Conceptualization, Supervision, Validation, Writing – review & editing.

Declaration of competing interest

The authors declare that they have no known competing financial interests or personal relationships that could have appeared to influence the work reported in this paper.

Acknowledgements

None.

Appendix A. Supplementary data

Supplementary data to this article can be found online at https://doi.org/10.1016/j.heliyon.2024.e25463.

Abbreviations

GC	gastric cancer
TCGA	The Cancer Genome Atlas
GEO	Gene Expression Omnibus
TCIA	The Cancer Immunome Atlas
DEGs	differentially expressed genes
DEIRGs	differentially expressed immune related genes
DEMRGs	differentially expressed metabolism related genes
KEGG	Kyoto Encyclopedia of Genes and Genomes
KM	Kaplan-Meier
LASSO	least absolute shrinkage and selection operator
ROC	receiver operating characteristic
AUC	area under curve
FDR	False Discovery Rate
AIC	Akaike information criterion
RS	risk score
HR	high risk
LR	low risk
OS	overall survival
GSVA	Gene Set Variation Analysis
ESTIMATE	Estimation of STromal and Immune cells in MAlignant Tumor tissues using Expression data
GSEA	Gene Set Enrichment Analysis
ssGSEA	single sample gene set enrichment analysis
ECM	extracellular matrix
EMT	epithelial-mesenchymal transition
IPS	immunophenoscore
ICI	immune cells infiltration
ICIs	immune checkpoint inhibitors
CAFs	cancer associated fibroblasts
TME	tumor microenvironment
TMB	tumor mutation burden
Tregs	Regulatory T cells

References

[1] D.Y. Oh, L. Fong, E.W. Newell, M.J. Turk, H. Chi, H.Y. Chang, A.T. Satpathy, B. Fairfax, B. Silva-Santos, O.J.C.C. Lantz, Toward a better understanding of T cells in cancer 39 (12) (2021) 1549–1552.

[2] A. Durgeau, Y. Virk, S. Corgnac, Mami-Chouaib Fjfii, Recent advances in targeting CD8 T-cell immunity for more effective cancer immunotherapy 9 (2018) 14.

[3] H. Zhang, Z. Zhu, S. Modrak, Little AJTJoI, Tissue-resident memory CD4+ T cells play a dominant role in the initiation of antitumor immunity 208 (12) (2022) 2837–2846.

[4] A. Cachot, M. Bilous, Y.-C. Liu, X. Li, M. Saillard, M. Cenerenti, G.A. Rockinger, T. Wyss, P. Guillaume, JJSa Schmidt, Tumor-specific cytolytic CD4 T cells mediate immunity against human cancer 7 (9) (2021) eabe3348.

[5] E. Seung, Z. Xing, L. Wu, E. Rao, V. Cortez-Retamozo, B. Ospina, L. Chen, C. Beil, Z. Song, B.J.N. Zhang, A trispecific antibody targeting HER2 and T cells inhibits breast cancer growth via CD4 cells 603 (7900) (2022) 328–334.

[6] H. Jonuleit, Schmitt EJTJoI, The regulatory T cell family: distinct subsets and their interrelations 171 (12) (2003) 6323–6327.

[7] Y. Ohue, Nishikawa HJCs: regulatory T (Treg) cells in cancer: can Treg cells be a new therapeutic target? 110 (7) (2019) 2080–2089.

[8] A. Tanaka, Sakaguchi Sjejoi, Targeting Treg cells in cancer immunotherapy 49 (8) (2019) 1140–1146.

[9] J. Huo, W. Xie, X. Fan, PJCiB. Sun, Medicine, Pyroptosis, apoptosis, and necroptosis molecular subtype derived prognostic signature universal applicable for gastric cancer-A large sample and multicenter retrospective analysis 149 (2022) 106037.

[10] X. Huang, H. Hu, J. Liu, X. Zhang, Y. Jiang, L. Lv, S.J.C.B. Du, Biophysics: immune analysis and small molecule drug prediction of hepatocellular carcinoma based on single sample gene set enrichment analysis 80 (2) (2022) 427–434.

[11] K. Yoshihara, M. Shahmoradgoli, E. Martínez, R. Vegesna, H. Kim, W. Torres-Garcia, V. Treviño, H. Shen, P.W. Laird, Levine DAJNc: Inferring tumour purity and stromal and immune cell admixture from expression data 4 (1) (2013) 2612.

[12] S. Hänzelmann, R. Castelo, Guinney Jjbb, GSVA, gene set variation analysis for microarray and RNA-seq data 14 (2013) 1–15.

[13] A. Mayakonda, D.-C. Lin, Y. Assenov, C. Plass, Koeffler Hpjgr, Maftools: efficient and comprehensive analysis of somatic variants in cancer 28 (11) (2018) 1747–1756.

[14] S. Liu, Z. Wang, R. Zhu, F. Wang, Y. Cheng, Y.J.J. Liu, Three differential expression analysis methods for RNA sequencing: limma, EdgeR, DESeq2. (175) (2021) e62528.

[15] G. Yu, L.-G. Wang, Y. Han, He Q-YJOajoib: clusterProfiler: an R package for comparing biological themes among gene clusters 16 (5) (2012) 284–287.

[16] A. Subramanian, P. Tamayo, V.K. Mootha, S. Mukherjee, B.L. Ebert, M.A. Gillette, A. Paulovich, S.L. Pomeroy, T.R. Golub, Lander ESJPotNAoS, Gene set enrichment analysis: a knowledge-based approach for interpreting genome-wide expression profiles 102 (43) (2005) 15545–15550.
[17] K.P. Sinaga, M-SJIa Yang, Unsupervised K-means clustering algorithm 8 (2020) 80716–80727.
[18] H.J.P. Bozdogan, Model selection and Akaike's information criterion (AIC): the general theory and its analytical extensions 52 (3) (1987) 345–370.
[19] J. Huo, J. Cai, L.J.C.M. Wu, Comprehensive analysis of metabolic pathway activity subtypes derived prognostic signature in hepatocellular carcinoma 12 (1) (2023) 898–912.
[20] P. Charoentong, F. Finotello, M. Angelova, C. Mayer, M. Efremova, D. Rieder, H. Hackl, Trajanoski Zjcr, Pan-cancer immunogenomic analyses reveal genotype-immunophenotype relationships and predictors of response to checkpoint blockade 18 (1) (2017) 248–262.
[21] D. Maeser, R.F. Gruener, Huang RSJBib, oncoPredict: an R package for predicting in vivo or cancer patient drug response and biomarkers from cell line screening data 22 (6) (2021) bbab260.
[22] TAJNm Waldmann, Immunotherapy: past, present and future 9 (3) (2003) 269–277.
[23] D. Fukumura, J. Kloepper, Z. Amoozgar, D.G. Duda, Jain RKJNrCo, Enhancing cancer immunotherapy using antiangiogenics: opportunities and challenges 15 (5) (2018) 325–340.
[24] R.E. Tay, E.K. Richardson, Toh HCJCgt, Revisiting the role of CD4+ T cells in cancer immunotherapy—new insights into old paradigms 28 (1–2) (2021) 5–17.
[25] J. Borst, T. Ahrends, N. Bąbała, C.J. Melief, W.J.N.R.I. Kastenmüller, CD4+ T cell help in cancer immunology and immunotherapy 18 (10) (2018) 635–647.
[26] P. Muranski, Restifo Npjcoii, Adoptive immunotherapy of cancer using CD4+ T cells 21 (2) (2009) 200–208.
[27] D.Y. Oh, L.J.I. Fong, Cytotoxic CD4+ T cells in cancer: expanding the immune effector toolbox 54 (12) (2021) 2701–2711.
[28] E. Tran, S. Turcotte, A. Gros, P.F. Robbins, Y.-C. Lu, M.E. Dudley, J.R. Wunderlich, R.P. Somerville, K. Hogan, C.S.J.S. Hinrichs, Cancer immunotherapy based on mutation-specific CD4+ T cells in a patient with epithelial cancer 344 (6184) (2014) 641–645.
[29] M. Binnewies, A.M. Mujal, J.L. Pollack, A.J. Combes, E.A. Hardison, K.C. Barry, J. Tsui, M.K. Ruhland, K. Kersten, M.A.J.C. Abushawish, Unleashing type-2 dendritic cells to drive protective antitumor CD4+ T cell immunity, e516 177 (3) (2019) 556–571.
[30] A. Granito, et al., Hepatocellular carcinoma in viral and autoimmune liver diseases: role of CD4+ CD25+ Foxp3+ regulatory T cells in the immune microenvironment 27 (22) (2021) 2994.